

# Influence of LA and GA Sequence in the PLGA Block on the Properties of Thermogelling PLGA-PEG-PLGA Block Copolymers

Lin Yu, Zheng Zhang, and Jiandong Ding\*

Key Laboratory of Molecular Engineering of Polymers of Ministry of Education, Department of Macromolecular Science, Laboratory of Advanced Materials, Fudan University, Shanghai 200433, China

**ABSTRACT:** This paper reports the influence of sequence structures of block copolymers composed of poly(lactic acid-*co*-glycolic acid) (PLGA) and poly(ethylene glycol) (PEG) on their thermogelling aqueous behaviors. A series of thermogelling PLGA-PEG-PLGA triblock copolymers with similar chemical compositions and block lengths but different sequences of D,L-lactide (LA) and glycolide (GA) in the PLGA block were synthesized. The difference of sequence structures arises from the different reactivities of LA and GA during the copolymerization and the transesterification after polymerization. The sol–gel transition temperature and height of gel window were found to be regulated by the sequence structure. Our study reveals that the macromolecular sequence structure influences the hydrophobic/hydrophilic balance of this kind of amphiphilic copolymers and thus alters mesoscopic micellization and the forthcoming macroscopic physical gelation in water. This finding might be helpful to guide the molecular design of the underlying thermogelling systems as injectable hydrogels.



## ■ INTRODUCTION

In situ gelling materials can be injected into the body and then solidified under physiological conditions.<sup>1–11</sup> Especially, inverse thermogelling copolymers with the sol–gel transition upon increase of temperature have attracted interest due to their ease of administration, avoidance of organic solvents, and minimal invasiveness.<sup>3–5,11–21</sup> It has been known that those polymers should be amphiphilic with a delicate balance between hydrophobicity and hydrophilicity.<sup>22,23</sup> Typically, biodegradable thermogelling polymers are block copolymers composed of poly(ethylene glycol) (PEG) and poly(lactic acid-*co*-glycolic acid) (PLGA),<sup>24–26</sup> PEG and poly(lactic acid) (PLA),<sup>27,28</sup> PEG and poly(caprolactone) (PCL),<sup>29,30</sup> PEG and poly( $\epsilon$ -caprolactone-*co*-D,L-lactic acid) (PCLA),<sup>31–33</sup> PEG and poly(propylene fumarate),<sup>34</sup> PEG/poly(propylene glycol)/polyester,<sup>35,36</sup> PEG/polypeptide,<sup>37,38</sup> PEG/polyester/polypeptide,<sup>39,40</sup> poly(phosphazenes),<sup>41,42</sup> etc.

Among those thermogelling polymers, PEG/PLGA block copolymers are very useful for drug delivery, tissue regeneration, cell therapy, and wound healing.<sup>43–48</sup> For instance, in vitro studies showed that the release of paclitaxel, an anticancer agent, can last for up to 50 days from the thermoreversible PLGA-PEG-PLGA hydrogel (ReGel).<sup>43</sup> In comparison with the commercial paclitaxel product Taxol, ReGel/paclitaxel formulation exhibited high efficacy against human breast tumor xenografts (MDA231). An advanced stage of the clinical trial of this formulation (OncoGe) is ongoing.<sup>48</sup> Our group confirmed the sustained release of PEGylated camptothecin (CPT) from the PLGA-PEG-PLGA hydrogel for over 1 month and satisfactory anticancer efficacy in mice.<sup>46</sup> Jeong et al. demonstrated that the cartilage defect can be notably repaired using the mixture of thermogelling PLGA-g-PEG aqueous solutions and chondrocyte suspensions.<sup>44</sup>

Meanwhile, both *in vitro* and *in vivo* studies revealed that the above copolymers showed good biocompatibility.<sup>21,43</sup>

The gelation and degradation behaviors of thermogelling PEG/PLGA block copolymers can be controlled by many internal factors such as molecular weight (MW) of polymers, block ratio, concentration, and end group<sup>22,24,25,49,50</sup> and can also be affected by external additives such as PEG homopolymers or salts.<sup>24,26,51</sup> By adding a typical salt-in consolute, for instance, NaSCN, the sol–gel transition shifts to a high temperature; conversely, addition of a salt-out consolute, e.g., NaCl, leads to the decrease in sol–gel transition temperature.<sup>24</sup> With a given PEG block, the sol–gel transition temperature and critical gel concentration (CGC) also decrease with the increase of MW of PLGA block or LA/GA ratio.<sup>24,25</sup> The PLGA block is usually synthesized by ring-opening copolymerization (ROP) of D,L-lactide (LA) and glycolide (GA) in the presence of catalyst, for instance, stannous octoate. ROP of an LA leads to two consecutive repeated units of lactic acid (L), while ROP of a GA leads to two consecutive repeated units of glycolic acid (G).

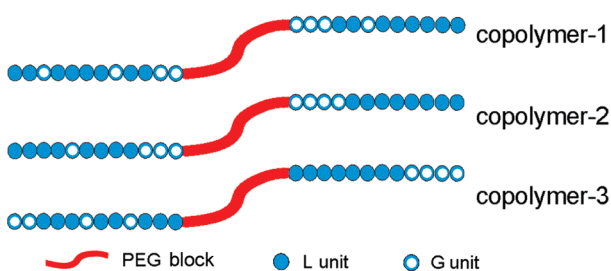
In general, the sequence structures of PLGA or similar polyester chains are modulated by the kind of applied initiators as well as by transesterification occurring in the ROP.<sup>31,52–54</sup> It is thought that the transesterification results in the “random” distribution of comonomer units along the polymer chains. However, the extent of randomness and the possible effects of sequence structures on thermogelling behaviors remain as open questions. In this study, we synthesized a series of thermogelling PLGA-PEG-PLGA triblock copolymers with similar chemical compositions and block lengths but different sequences of units of L and G in the PLGA

**Received:** December 27, 2010

**Revised:** January 31, 2011

**Published:** March 01, 2011

**Scheme 1. Schematic Presentation of Sequence Structures of PLGA-PEG-PLGA Triblock Copolymers Obtained via Different Polymerization Conditions<sup>a</sup>**



<sup>a</sup> ROP of LA and GA is initiated by the hydroxy groups of the ends of PEG block. Due to much higher reactivity of GA than LA, the copolymerization of LA and GA leads to a tapered distribution with the G units close to PEG block in copolymer-1 and copolymer-2. The difference of these two copolymers comes from different synthesis temperatures, which influence transesterification. In synthesis of copolymer-3, LA is added before GA resulting in LA-GA blocks, with a bit of randomness also due to transesterification.

block as schematically presented in Scheme 1. The different sequence structures of PLGA blocks will be achieved via controlling conditions in ROP of LA and GA initiated by PEG. The block structure will be characterized and the effect of sequence structures on the macroscopic aqueous behavior will be discussed as well.

## EXPERIMENTAL SECTION

**Materials.** Polyethylene glycol (PEG, MW 1500) and stannous 2-ethylhexanoate (stannous octoate, 95%) were purchased from Sigma. The end groups of PEG are hydroxyl. LA and GA were acquired from Purac and used as received. All other chemicals were of reagent grade and used as received.

**Synthesis of PLGA-PEG-PLGA Triblock Copolymers.** Triblock copolymers PLGA-PEG-PLGA (copolymer-1) were prepared following typical ROP of LA and GA using hydroxyl-terminated PEG as initiator. Briefly, 15 g of PEG (0.01 mol) was put into a dry three-necked flask and then dried under vacuum with continuous stirring at 150 °C for 4 h. Under the protection of argon, LA (0.212 mol) and GA (0.014 mol) with 15/1 molar ratio were added and stirred under reduced pressure at 120 °C for 30 min. The flask was replaced with argon at least three times to remove the moisture in monomers within the duration. After all the monomers melted, the initiator, stannous octoate (0.2 wt % of monomers), was added. Finally, the reaction proceeded with continuous stirring at 160 °C for 12 h under an argon atmosphere. Then, a vacuum was used to remove unreacted monomers in the reaction mixture for 60 min. The obtained crude polymers were dissolved in cold water (4–8 °C). After completely dissolving, the polymer solution was heated to 80 °C to precipitate the polymer products and remove water-soluble low-MW polymers and unreacted monomers. The precipitated polymer was separated from the supernatant by decantation. The above process was repeated twice to obtain the copolymer, and the residual water in the copolymer was removed by lyophilization. The yield of the final product was about 80%.

Similarly, the polymerization of copolymer-2 was carried out at 130 °C for 12 h. The polymerization of copolymer-3 was carried out by a two-step approach. First, the polymerization reaction happened in the presence of PEG, LA, and stannous octoate at 130 °C for 8 h; then GA and stannous octoate were added, and the reaction continued at 130 °C for 4 h more.

To further investigate the influence of polymerization conditions, a given amount of purified copolymer-3 (10 g) was transferred into a

reaction vessel and then heated to 160 °C for 12 h. After purification, we obtained the product, which was called copolymer-4.

**NMR Characterization.** To confirm the chemical structure and composition of the copolymers, <sup>1</sup>H NMR measurements of the samples in CDCl<sub>3</sub> were performed in a 500 MHz proton NMR spectrometer (Bruker, DMX500 spectrometer). <sup>55</sup> <sup>1</sup>H NMR spectra were recorded to examine the spectra of copolymer-2 in D<sub>2</sub>O (20 wt %) as a function of temperature. The solution temperature was equilibrated for 20 min before the measurement. Chemical shifts were referred to the solvents (7.26 ppm for CDCl<sub>3</sub> and 4.70 ppm for D<sub>2</sub>O).

**Gel Permeation Chromatography.** Molecular weights and their distributions of copolymers were determined by gel permeation chromatography (GPC) on an Agilent1100 GPC system, which was equipped with a differential refractometer as detector. Tetrahydrofuran (THF) was used as the eluent at 35 °C at a flow rate of 1.0 mL/min. The MWs were calibrated with polystyrene (PS) standards.

**Sol–Gel Transition.** The sol–gel transition temperature was determined via the test tube inverting approach.<sup>23</sup> Each sample with a given concentration was prepared by dissolving the polymer in distilled water in a 2 mL vial and stored at 4 °C. The vials containing 0.5 mL polymer solutions were immersed in a water bath at designated temperature for 15 min. The sample was regarded as a “gel” in the case of no visual flow within 30 s by inverting the vial with a temperature increment of 1 °C per step.

**Rheological Analysis.** The sol–gel transition of the copolymer aqueous solutions (15 wt %) was also investigated on a strain-controlled rheometer (ARES Rheometric Scientific) using a Couette cell (Couette diameter, 34 mm; bob diameter, 32 mm; bob height, 33.3 mm; bob gap, 2 mm). Cold polymer solutions were carefully transferred into the Couette cell and overlaid with a thin layer of low-viscosity silicone oil to minimize solvent evaporation. During temperature-sweep experiments, an appropriate strain amplitude was set according to preliminary tests to get both the linearity of viscoelasticity and sufficient torque for data collection. Temperature was controlled with an accuracy of ±0.05 °C (Neslab, RTE-130). Temperature scans with a fixed angular frequency  $\omega$  of 10 rad/s were carried out at a heating rate of 0.5 °C/min. The frequency and heating rate were also pre-evaluated to be appropriate.

**Determination of Critical Micelle Concentration.** The hydrophobic dye solubilization method was used to determine the critical micelle concentration (CMC) at room temperature. The solution of 1,6-diphenyl-1,3,5-hexatriene (DPH) in methanol (10  $\mu$ L at 0.4 mM) was added into an aqueous polymer solution (1 mL) with concentrations from 0.001 to 0.2 wt % and equilibrated overnight at 4 °C. The absorption spectra of the sample in the range 320–420 nm were recorded at various concentrations using a UV–vis spectrophotometer. The CMC value was determined from the plot of the difference of absorbance at 378 and 400 nm ( $A_{378} - A_{400}$ ) versus logarithmic concentration.

**Dynamic Light Scattering.** Dynamic light scattering (DLS) measurements were carried out in a laser scattering spectrophotometer (Autosizer 4700, Malvern) using a vertically polarized incident beam at 532 nm supplied by an argon ion laser. The scattering angle of measurements was set at 90°. The sample was filtered through a 0.45  $\mu$ m filter (Millipore) to remove dust before measurement. The hydrodynamic radiiuses of particles were calculated following the Stokes–Einstein equation. The intensity–intensity time correction function was analyzed by the CONTIN method.

## RESULTS AND DISCUSSION

**Microscopic Chemical Structures of Synthesized Copolymers.** PLGA-PEG-PLGA triblock copolymers were synthesized via ROP of GA and LA in the presence of PEG using Sn(Oct)<sub>2</sub> as a catalyst. The polymerization was conducted in bulk with continuous stirring. The <sup>1</sup>H NMR spectrum of a PLGA-PEG-PLGA

triblock copolymer is shown in Figure 1. In a method similar to that of Jeong et al.,<sup>55</sup> the number average MW of the PLGA-PEG-PLGA triblock copolymer was determined by the NMR peaks of 1.55, 3.60, and 4.80 ppm. Four samples were obtained under different polymerization conditions. The calculated MW values are listed in Table 1.

According to Gilding and Reed,<sup>56</sup> the reactivity ratios of LA and GA are  $r_L = 0.2$  and  $r_G = 2.8$  at 200 °C, respectively. Therefore, the reactivity ratio of LA is by a long way lower than that of GA. When the GA and LA were copolymerized at 130 or 160 °C, the ring of GA was preferentially opened and linked to the hydroxy end groups of the PEG block in the first step of copolymerization. With longer polymerization time, LA was built in polymer chains when GA was depleted. Transesterification in the polymerization process made the redistribution of sequences in the polyester chain, resulting in the change of sequence structure and even the length distribution of PLGA blocks. Generally, transesterification reaction depends on reaction temperature and time.<sup>52,54,57</sup> The

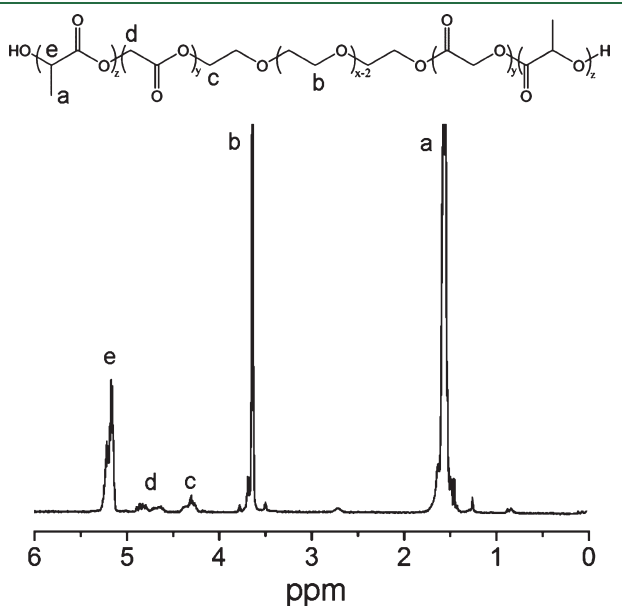


**Figure 1.**  $^1\text{H}$  NMR spectrum of PLGA-PEG-PLGA triblock copolymer-1 in  $\text{CDCl}_3$ .

temperature is higher and the time is longer, the stronger transesterification is, which results in the more random sequence.

While the large peaks in the whole  $^1\text{H}$  NMR spectra of our samples are similar, some relatively small peaks are different. Next, we specifically pay attention to the proton signals of  $-\text{CH}_2-$  of the repeated unit G (peak d in Figure 1) and ethylene

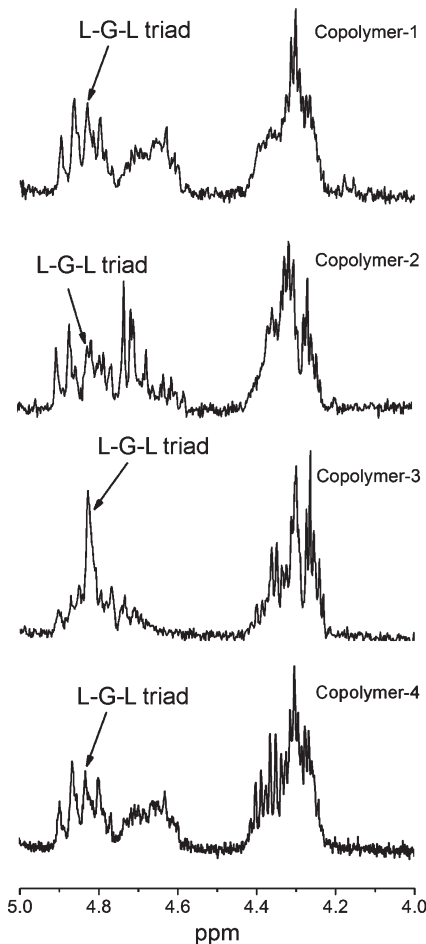


**Figure 2.**  $^1\text{H}$  NMR spectra of the proton peaks of  $-\text{CH}_2-$  of G units and ethylene glycol units neighboring the PLGA block for the indicated copolymers.

**Table 1.** PLGA-PEG-PLGA Triblock Copolymers Synthesized in This Study

sample	synthesis condition	block length	$\text{PEG } M_n^a$	$M_n^a$	$M_n^b$	$(M_w/M_n)^b$
copolymer-1	adding LA and GA simultaneously; reacting at 160 °C for 12 h	theoretical: $(\text{LA/GA})_{21.2/1.4}-(\text{EG})_{34}-(\text{LA/GA})_{21.2/1.4}$ experimental: $(\text{LA/GA})_{22.4/1.6}-(\text{EG})_{34}-(\text{LA/GA})_{22.4/1.6}$	1500	4910	6520	1.21
copolymer-2	adding LA and GA simultaneously; reacting at 130 °C for 12 h	theoretical: $(\text{LA/GA})_{21.2/1.4}-(\text{EG})_{34}-(\text{LA/GA})_{21.2/1.4}$ experimental: $(\text{LA/GA})_{21.8/1.4}-(\text{EG})_{34}-(\text{LA/GA})_{21.8/1.4}$	1500	4800	6640	1.18
copolymer-3	first, LA at 130 °C for 8 h; then GA at 130 °C for 4 h more	theoretical: $(\text{LA/GA})_{21.2/1.4}-(\text{EG})_{34}-(\text{LA/GA})_{21.2/1.4}$ experimental: $(\text{LA/GA})_{21.8/1.5}-(\text{EG})_{34}-(\text{LA/GA})_{21.8/1.5}$	1500	4810	6540	1.12
copolymer-4	heating some copolymer-3 to 160 °C and lasting for 12 h	theoretical: $(\text{LA/GA})_{21.8/1.5}-(\text{EG})_{34}-(\text{LA/GA})_{21.8/1.5}$ experimental: $(\text{LA/GA})_{19.1/1.5}-(\text{EG})_{34}-(\text{LA/GA})_{19.1/1.5}$	1500	4420	5130	1.21

<sup>a</sup> The number-average MW,  $M_n$ , of the central block PEG was provided by Aldrich.  $M_n$  of each copolymer was calculated by  $^1\text{H}$  NMR. <sup>b</sup> Measured via GPC, relative to PS standards.

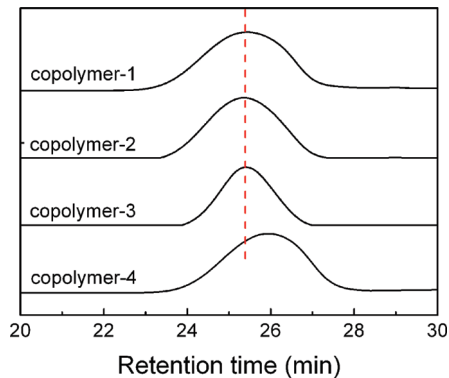


**Figure 3.** GPC traces of the four samples. The dashed line indicates the similar peaks and thus similar MWs for copolymer-1, copolymer-2, and copolymer-3.

glycol (EG) neighboring the PLGA block (peak c in Figure 1), as shown in Figure 2. The peak at 4.83 ppm was assigned to the signal of  $-\text{CH}_2-$  of the L-G-L sequence according to the previous report.<sup>52</sup> The L-G-L triad cannot occur in ROP reaction because GA is composed of two consecutive G units. Therefore, Figure 2 confirms the existence of transesterification. Compared with that of copolymer-2, the more remarkable transesterification in copolymer-1 verifies that the transesterification depends on the polymerization temperature. Interestingly, the extent of transesterification in copolymer-3 is not low. During the preparation of copolymer-3, only LA was added and polymerized in the presence of PEG in the first step of polymerization at 130 °C. After reaction for 8 h, GA was added and polymerized at 130 °C for 4 h more. So, PLA-PEG-PLA triblock copolymers were obtained in the first step and then copolymer-3 was finally synthesized by polymerizing GA in the presence of PLA-PEG-PLA. A quick transesterification reaction must occur in the second step of polymerization, resulting in the formation of L-G-L sequences. A similar phenomenon was observed in synthesis of poly( $\epsilon$ -caprolactone-*co*-glycolic acid) copolymers.<sup>58</sup>

To further confirm the influence of transesterification, a given amount of copolymer-3 was heated to 160 °C for 12 h and the obtained specimen was called copolymer-4. Copolymer-4 was characterized by <sup>1</sup>H NMR, and the change in proton signals of  $-\text{CH}_2-$  of G units was observed. The typical peaks of G units of copolymer-4 were different from those of copolymer-3, but similar to those of copolymer-1 in Figure 2. The result distinctly indicates that the change comes from the transesterification.

The basic data of the resultant triblock copolymers, including MWs, polydispersity, and compositions measured by <sup>1</sup>H NMR and GPC in this study, are summarized in Table 1. All of the GPC traces of four samples are unimodal with polydisperse index ( $M_w/M_n$ ) less than 1.21, reflecting that the purity is sufficiently high to study their physical properties (Figure 3). Interestingly, Figure 3 shows a decrease of polydispersity from copolymer-1 to copolymer-3, indicating that the polydispersity is also influenced by polymerization conditions. Compared with that of copolymer-3, the polydispersity of copolymer-4 increased, which was attributed to the transesterification. Meanwhile, copolymer-4 showed a reduced mean MW, reflecting that a bit of degradation also happened during the process of postpolymerization heating. The products obtained were basically reproducible by controlling the polymerization condition. In the following study, we focus on

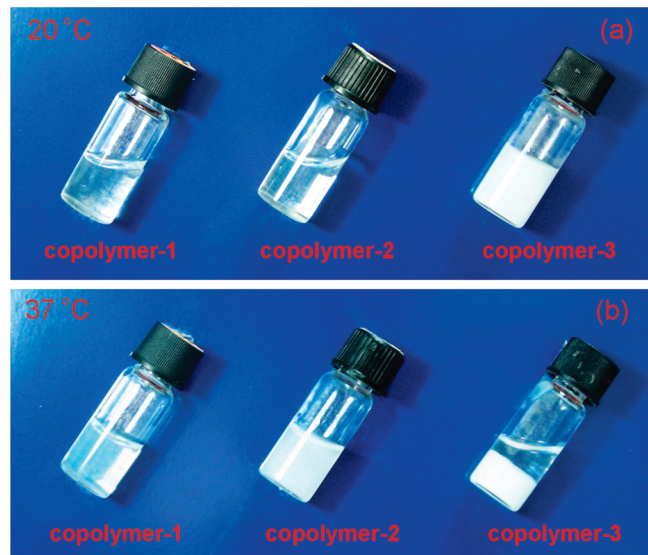


**Figure 4.** Images of polymeric aqueous systems exhibiting sol, sol, and gel states at 20 °C (a), and translucent gel, opaque gel, and precipitate states at 37 °C (b) for copolymer-1, copolymer-2, and copolymer-3, respectively. Concentration: 15 wt %. The chemical compositions of copolymer-1, copolymer-2 and copolymer-3 are indicated in Table 1.

copolymers 1–3 with similar MWs to investigate their thermogelling aqueous behaviors.

**Macroscopic Phase Behaviors of Concentrated Polymeric Aqueous Systems.** After the obtained copolymers (sample 1, 2, or 3) were mixed with water, significantly different states were observed at room temperature (20 °C) and body temperature (37 °C), as presented in Figure 4. Copolymer-1 and copolymer-2 were sols in water, whereas copolymer-3 exhibited a gel at 20 °C (Figure 4a). At 37 °C, copolymer-1 was a translucent gel while copolymer-2 took on an opaque gel. In contrast, copolymer-3 precipitated in water at the same temperature (Figure 4b). This finding indicates that the sequence structures of PLGA blocks in the copolymers have a significant influence on their aqueous behaviors, which can even determine whether or not the material is appropriate as an injectable biomedical hydrogel.

The phase diagrams of polymer aqueous solutions are shown in Figure 5. All of the three copolymers underwent sol–gel–precipitate transition with an external heat stimulus. The sol–gel transition temperatures seemed relatively less sensitive to concentration in the gel window, while the gel–precipitate transition temperatures were significantly dependent upon polymer concentration. From copolymer-1 to copolymer-3, the gel window shifted to the low temperature region, and the sol–gel transition temperatures decreased even about 20 °C. These results suggest that the global hydrophobicity of copolymers increases from copolymer-1 to copolymer-2 and to copolymer-3.

Dynamic rheological measurements were carried out to investigate the changes of modulus ( $G'$ ) and viscosity ( $\eta$ ) during hydrogel formation. The temperature dependence of  $G'$  and  $\eta$  for PLGA-PEG-PLGA aqueous solutions is shown in Figure 6. At low temperature, the samples were flowing liquids with a low viscosity, suggesting the good injectability of our material. In fact, both copolymer-1 and copolymer-2 can be conveniently administered by a 23-gauge needle. As the temperature increased, triblock copolymers underwent a significant modulus change. Usually, the abrupt increase of  $G'$  corresponds to the sol–gel

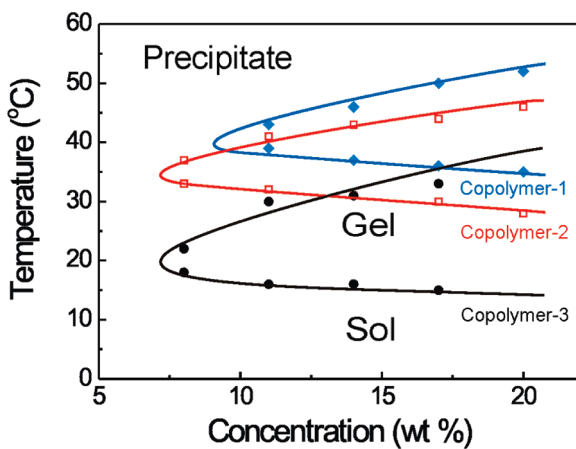


**Figure 5.** Phase diagrams of the aqueous systems of indicated copolymers. The transition temperatures were measured by the vial inverting approach. The resol state at high temperatures was actually a turbid suspension and the polymers were eventually precipitated.

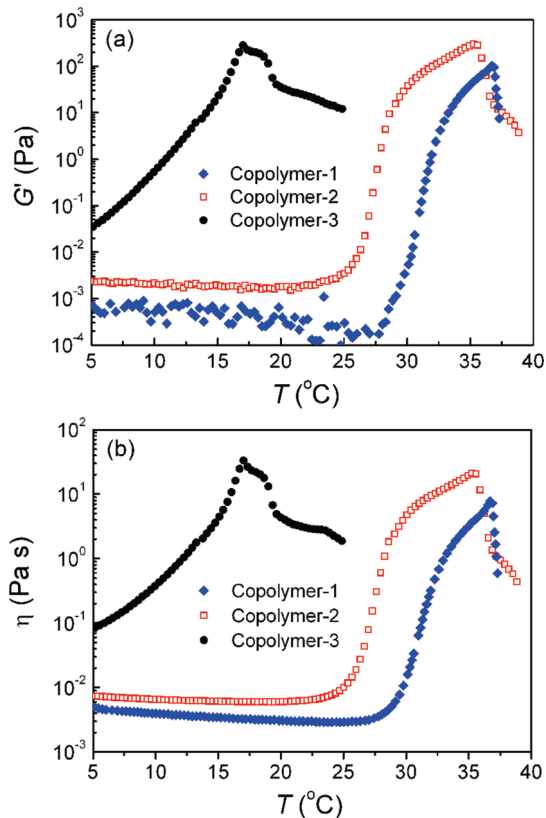


**Figure 6.** Storage modulus  $G'$  (a) and viscosity  $\eta$  (b) of samples with the indicated copolymers in aqueous solutions (15 wt %) as a function of temperature. Heating rate: 0.5 °C/min. Oscillatory frequency: 10 rad/s. There was no experimental data for copolymer-3 at high temperatures, because polymers were precipitated under this circumstance.

transition. The transition temperature determined via rheological measurements (Figure 6) is very consistent with the transition temperature determined via the test inverting approach with a temperature increment of 1 °C per step and each point equilibrated for 15 min (Figure 5), indicating the achievement of thermal equilibrium in the current heating rate (0.5 °C/min)

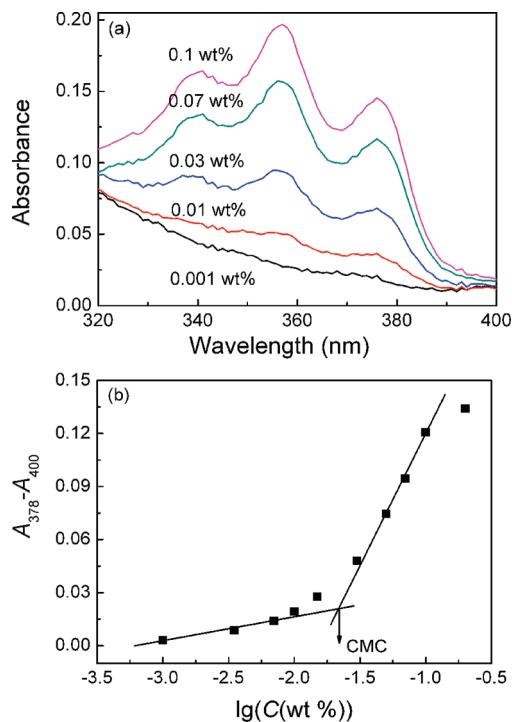


**Figure 7.** (a) UV-vis spectra of copolymer-2 aqueous solutions containing the hydrophobic dye, DPH. The dye concentration was fixed at 4  $\mu$ M and polymer concentration varied. For clarity, just five weight concentrations are shown in (a). (b) Determination of CMC of copolymer-2 in water by extrapolation of the difference of absorbance at 378 and 400 nm.

in our rheological tests. In examination of the transition temperature of thermogelling PLGA-g-PEG aqueous solution via dynamic rheological measurements with different heating rates of 0.2, 0.5, and 1 °C/min, the Jeong group also confirmed that even 1.0 °C/min was an appropriate heating rate.<sup>26</sup> It seems helpful for indicating that a frequency-dependent analysis is also meaningful for investigation of viscoelasticity of a thermoreversible hydrogel.<sup>59</sup> The frequency used in Figure 6 is appropriate to reflect a sol–gel transition. The different rheological behaviors of three samples upon increase of temperature in Figure 6 further confirm that the sequence structures of copolymers can significantly modulate the sol–gel transition temperatures.

**Mesoscopic Self-Assembly of Amphiphilic Copolymers in Water.** The micellization of the PLGA-PEG-PLGA triblock copolymer in water was examined by the hydrophobic dye method. As the polymer concentration increased, the PLGA-PEG-PLGA triblock copolymers in water would self-assemble into a core–corona structure, and the hydrophobic dye DPH would be partitioned into the hydrophobic cores of micelles, resulting in the increased absorption at 320–400 nm as a characteristic triplet band (Figure 7a). The crossing point of two extrapolated lines was used to determine CMC (Figure 7b). The CMC values of three samples at 25 °C were in a range of 0.1–0.3 mg/mL.

The change in the micelle size and distribution of copolymer-2 with concentration was detected via DLS (Figure 8). At a low concentration (0.1 wt %), the micelles only showed a single-peak profile. When the concentration was 0.5 wt %, some micelles were aggregated to large particles of 80–200 nm while the population of 21 nm micelles was still dominant. When the concentration was

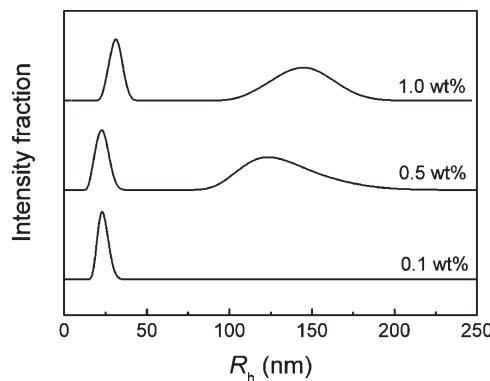


**Figure 8.** Distribution of hydrodynamic radius of micelles in aqueous solutions (copolymer-2) at indicated concentrations measured by DLS at 20 °C.

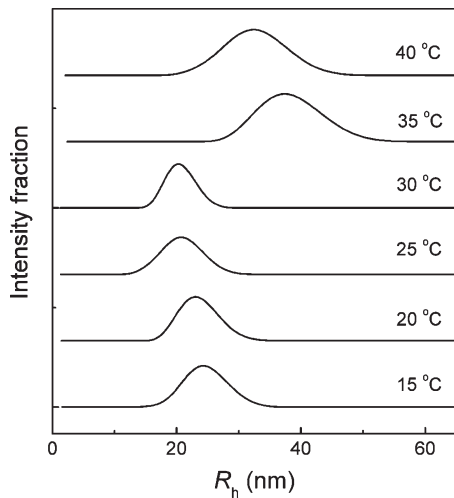


**Figure 9.** Distribution of hydrodynamic radius  $R_h$  of micelles of copolymer-2 in water (0.1 wt %) at indicated temperatures.

increased to 1.0 wt %, the average radius of micelles was raised to 31 nm and coexisted with the larger micellar aggregates.

Further, the micelle size and distribution of PLGA-PEG-PLGA triblock copolymer aqueous solution at a low concentration were studied by DLS under various temperatures. As shown in Figure 9, the micelles exhibited unimodal size distributions at all examined temperatures. The micelles became smaller upon heating. Then, the significant increases of the micelle size and micelle size distribution were observed at 35 °C, which reflected the significant micelle aggregation. At a higher temperature (40 °C), the average radius of micelles decreased again. The shrinkage of the polymer aggregation with increasing temperature might owe to the partial dehydration of the PEG blocks.<sup>60</sup>

The average micelle sizes in 0.1 wt % aqueous solution as a function of temperature are shown in Figure 10. As the temperature increased, different profiles were observed among micellization behaviors for all the three copolymers, which illustrated that the self-assembly of the PLGA-PEG-PLGA block copolymers in water was very sensitive to the sequence structures.

Proton NMR was used to monitor the changes in the molecular environment of copolymers during the sol–gel transition. The <sup>1</sup>H NMR spectra of 20 wt % copolymer-2 in D<sub>2</sub>O at different temperatures are displayed in Figure 11. Chloroform is a

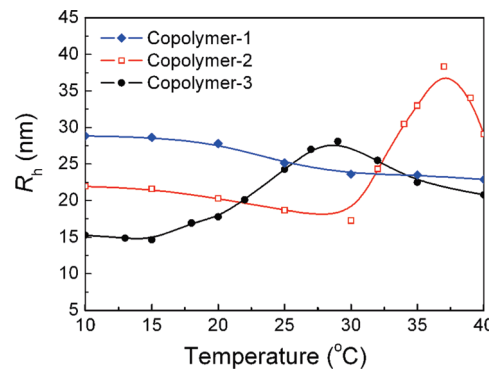


**Figure 10.** Hydrodynamic radius of micelles in aqueous solutions (0.1 wt %) as a function of temperature measured by DLS. The heating rate was 1 °C/min and the duration equilibrating each designated temperature was 15 min.

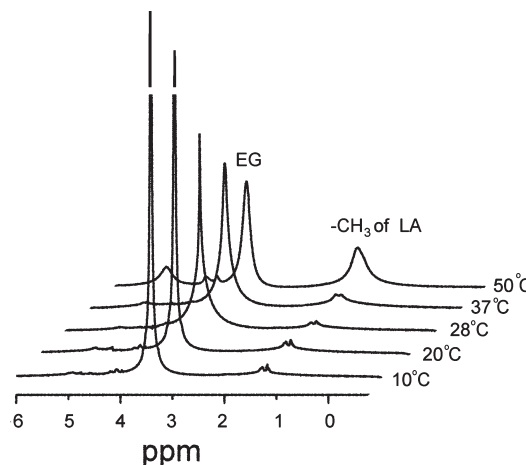


**Figure 11.** <sup>1</sup>H NMR spectra of 20 wt % copolymer-2 in D<sub>2</sub>O solution as a function of temperature. The solvent peak at 4.70 ppm was deleted to clearly observe the proton peak of the methylene group of PEG.

nonselective good solvent for all segments of the copolymer, whereas water is a good solvent for the PEG block but a poor solvent for the PLGA block. Both the proton signals of the methyl group of PLGA and the methylene group of PEG were observed as sharp peaks in CDCl<sub>3</sub> (Figure 1). In contrast, in D<sub>2</sub>O, the methyl proton signals of PLGA were broadened, whereas the signal of the methylene protons of PEG was observed as a sharp peak at 10 and 20 °C (sol state), confirming the formation of micelles with PLGA cores and PEG coronas in water. In the gel state (28 and 37 °C), the PEG peak was collapsed compared with that of the sol state (10 and 20 °C), whereas no obvious change in PLGA peak height was observed. These features indicated that the micelle structure was maintained during the sol–gel transition. Upon further increasing the temperature to 50 °C, an obvious increase of PLGA signal was observed, suggesting that the micellar structure of the polymers in the aqueous environment was destroyed.

**Hierarchical Self-Assembly of PLGA-PEG-PLGA Copolymers in Water.** According to our previous investigations, the temperature-induced sol–gel transition of PLGA-PEG-PLGA triblock copolymer in water is attributed to the micellar aggregation and the driving force of thermal gelation is the hydrophobic interaction.<sup>22,61</sup> DLS experiments (Figure 9) indicate the

micellar aggregation with the increase of temperature. This evidence together with the maintenance of micelle structure during sol–gel transition via NMR measurements (Figure 11) implies the formation of a percolated micelle network in the gel state in our case.

Our previous studies also found that with a fixed PEG block, the chain length and molecular composition of the PLGA block influence the thermogelling property of PLGA-PEG-PLGA tri-block copolymers in water.<sup>50,61</sup> The present study further illuminates the significant effect of sequence structure of PLGA block on the thermosensitivity of those triblock copolymers. The difference of the sequence structure among the copolymers is mainly ascribed to the transesterification in the polymerization process. The different sequence structures and polydispersities alter the global balance of hydrophobicity and hydrophilicity, which is critical to determine mesoscopic micellization of the amphiphilic block copolymers in water and further micellar percolation to form a macroscopic hydrogel.

## CONCLUSIONS

A series of PLGA-PEG-PLGA triblock copolymers were synthesized and characterized. The different polymerization conditions affected the sequence structure of the PLGA blocks in PLGA-PEG-PLGA triblock copolymers. The difference of sequence structure in the obtained copolymers was attributed to the differences of reactivity between LA and GA in ROP and the postpolymerization transesterification. The aqueous solutions of the PLGA-PEG-PLGA triblock copolymers in this study exhibited a temperature-induced sol–gel transition in water, and the gelling behaviors were found to be tunable by adjusting the sequence structure in the PLGA block. The effect of sequence structure on macroscopic physical gelation was confirmed to happen via influence of mesoscopic micellization in water. Our study highlights the importance of polymerization conditions including synthesis temperature in “random” copolymerization of two monomers with different reactivities, sheds more insight into the hierarchical self-assembly of this kind of amphiphilic copolymers in water, and enriches the strategy to design an injectable hydrogel.

## AUTHOR INFORMATION

### Corresponding Author

\*Tel.: 086-021-65643506. E-mail: jdding1@fudan.edu.cn.

## ACKNOWLEDGMENT

The group was supported by Chinese Ministry of Science and Technology (973 Program No. 2009CB930000), NSF of China (Grants No. 50903021 and No. 21034002), Science and Technology Developing Foundation of Shanghai (Grant No. 09ZR1403700), and the Specialized Research Fund for the Doctoral Program of Higher Education of China (SRFDP; No. 20090071120014).

## REFERENCES

- (1) Jeong, B.; Bae, Y. H.; Lee, D. S.; Kim, S. W. *Nature* **1997**, 388, 860–862.
- (2) Hiemstra, C.; Zhou, W.; Zhong, Z. Y.; Wouters, M.; Feijen, J. *J. Am. Chem. Soc.* **2007**, 129, 9918–9926.
- (3) Yu, L.; Ding, J. D. *Chem. Soc. Rev.* **2008**, 37, 1473–1481.
- (4) He, C. L.; Kim, S. W.; Lee, D. S. *J. Controlled Release* **2008**, 127, 189–207.
- (5) Joo, M. K.; Park, M. H.; Choi, B. G.; Jeong, B. *J. Mater. Chem.* **2009**, 19, 5891–5905.
- (6) Fairbanks, B. D.; Schwartz, M. P.; Bowman, C. N.; Anseth, K. S. *Biomaterials* **2009**, 30, 6702–6707.
- (7) Ossipov, D. A.; Piskounova, S.; Varghese, O. P.; Hilborn, J. *Biomacromolecules* **2010**, 11, 2247–2254.
- (8) Zhu, W.; Li, Y. L.; Liu, L. X.; Chen, Y. M.; Wang, C.; Xi, F. *Biomacromolecules* **2010**, 11, 3086–3092.
- (9) Takei, T.; Sato, M.; Ijima, H.; Kawakami, K. *Biomacromolecules* **2010**, 11, 3525–3530.
- (10) Buwalda, S. J.; Dijkstra, P. J.; Calucci, L.; Forte, C.; Feijen, J. *Biomacromolecules* **2010**, 11, 224–232.
- (11) Tsitsilianis, C. *Soft Matter* **2010**, 6, 2372–2388.
- (12) Madsen, J.; Armes, S. P.; Bertal, K.; Lomas, H.; MacNeil, S.; Lewis, A. L. *Biomacromolecules* **2008**, 9, 2265–2275.
- (13) Kim, H. K.; Shim, W. S.; Kim, S. E.; Lee, K. H.; Kang, E.; Kim, J. H.; Kim, K.; Kwon, I. C.; Lee, D. S. *Tissue Eng. Part A* **2009**, 15, 923–933.
- (14) Jeong, Y.; Joo, M. K.; Bahk, K. H.; Choi, Y. Y.; Kim, H. T.; Kim, W. K.; Lee, H. J.; Sohn, Y. S.; Jeong, B. *J. Controlled Release* **2009**, 137, 25–30.
- (15) Wang, W. X.; Liang, H.; Al Ghanami, R. C.; Hamilton, L.; Fraylich, M.; Shakesheff, K. M.; Saunders, B.; Alexander, C. *Adv. Mater.* **2009**, 21, 1809–1813.
- (16) Mortisen, D.; Peroglio, M.; Alini, M.; Eglin, D. *Biomacromolecules* **2010**, 11, 1261–1272.
- (17) Soontornworajit, B.; Zhou, J.; Zhang, Z. Y.; Wang, Y. *Biomacromolecules* **2010**, 11, 2724–2730.
- (18) Garber, J. C.; Hoffman, A. S.; Stayton, P. S. *Biomacromolecules* **2010**, 11, 1833–1839.
- (19) Ma, Z. W.; Nelson, D. M.; Hong, Y.; Wagner, W. R. *Biomacromolecules* **2010**, 11, 1873–1881.
- (20) Garty, S.; Kimelman-Bleich, N.; Hayouka, Z.; Cohn, D.; Friedler, A.; Pelleg, G.; Gazit, D. *Biomacromolecules* **2010**, 11, 1516–1526.
- (21) Yu, L.; Zhang, Z.; Zhang, H.; Ding, J. D. *Biomacromolecules* **2010**, 11, 2169–2178.
- (22) Yu, L.; Zhang, H.; Ding, J. D. *Angew. Chem.-Int. Ed.* **2006**, 45, 2232–2235.
- (23) Yu, L.; Zhang, Z.; Zhang, H.; Ding, J. D. *Biomacromolecules* **2009**, 10, 1547–1553.
- (24) Jeong, B.; Bae, Y. H.; Kim, S. W. *Macromolecules* **1999**, 32, 7064–7069.
- (25) Lee, D. S.; Shim, M. S.; Kim, S. W.; Lee, H.; Park, I.; Chang, T. Y. *Macromol. Rapid Commun.* **2001**, 22, 587–592.
- (26) Chung, Y. M.; Simmons, K. L.; Gutowska, A.; Jeong, B. *Biomacromolecules* **2002**, 3, 511–516.
- (27) Joo, M. K.; Sohn, Y. S.; Jeong, B. *Macromolecules* **2007**, 40, 5111–5115.
- (28) Nagahama, K.; Fujiura, K.; Enami, S.; Ouchi, T.; Ohya, Y. *J. Polym. Sci., Part A: Polym. Chem.* **2008**, 46, 6317–6332.
- (29) Hwang, M. J.; Suh, J. M.; Bae, Y. H.; Kim, S. W.; Jeong, B. *Biomacromolecules* **2005**, 6, 885–890.
- (30) Kim, M. S.; Hyun, H.; Seo, K. S.; Cho, Y. H.; Lee, J. W.; Lee, C. R.; Khang, G.; Lee, H. B. *J. Polym. Sci., Part A: Polym. Chem.* **2006**, 44, 5413–5423.
- (31) Jiang, Z. Q.; Deng, X. M.; Hao, J. Y. *J. Polym. Sci., Part A: Polym. Chem.* **2007**, 45, 4091–4099.
- (32) Kang, Y. M.; Lee, S. H.; Lee, J. Y.; Son, J. S.; Kim, B. S.; Lee, B.; Chun, H. J.; Min, B. H.; Kim, J. H.; Kim, M. S. *Biomaterials* **2010**, 31, 2453–2460.
- (33) Zhang, Z.; Lai, Y. X.; Yu, L.; Ding, J. D. *Biomaterials* **2010**, 31, 7873–7882.
- (34) Behravesh, E.; Shung, A. K.; Jo, S.; Mikos, A. G. *Biomacromolecules* **2002**, 3, 153–158.
- (35) Loh, X. J.; Goh, S. H.; Li, J. *Biomacromolecules* **2007**, 8, 585–593.

- (36) Loh, X. J.; Tan, Y. X.; Li, Z. Y.; Teo, L. S.; Goh, S. H.; Li, J. *Biomaterials* **2008**, *29*, 2164–2172.
- (37) Choi, Y. Y.; Joo, M. K.; Sohn, Y. S.; Jeong, B. *Soft Matter* **2008**, *4*, 2383–2387.
- (38) Nguyen, M. K.; Park, D. K.; Lee, D. S. *Biomacromolecules* **2009**, *10*, 728–731.
- (39) Huynh, D. P.; Nguyen, M. K.; Kim, B. S.; Lee, D. S. *Polymer* **2009**, *50*, 2565–2571.
- (40) Nagahama, K.; Imai, Y.; Nakayama, T.; Ohmura, J.; Ouchi, T.; Ohya, Y. *Polymer* **2009**, *50*, 3547–3555.
- (41) Lee, B. H.; Song, S. C. *Macromolecules* **2004**, *37*, 4533–4537.
- (42) Potta, T.; Chun, C.; Song, S. C. *Biomacromolecules* **2010**, *11*, 1741–1753.
- (43) Zentner, G. M.; Rathi, R.; Shih, C.; McRea, J. C.; Seo, M. H.; Oh, H.; Rhee, B. G.; Mestecky, J.; Moldoveanu, Z.; Morgan, M.; Weitman, S. J. *Controlled Release* **2001**, *72*, 203–215.
- (44) Jeong, B.; Lee, K. M.; Gutowska, A.; An, Y. H. H. *Biomacromolecules* **2002**, *3*, 865–868.
- (45) Pratoomsoot, C.; Tanioka, H.; Hori, K.; Kawasaki, S.; Kinoshita, S.; Tighe, P. J.; Dua, H.; Shakesheff, K. M.; Rose, F. *Biomaterials* **2008**, *29*, 272–281.
- (46) Yu, L.; Chang, G. T.; Zhang, H.; Ding, J. D. *Int. J. Pharm.* **2008**, *348*, 95–106.
- (47) Lee, S. J.; Bae, Y.; Kataoka, K.; Kim, D.; Lee, D. S.; Kim, S. C. *Polym. J.* **2008**, *40*, 171–176.
- (48) Elstad, N. L.; Fowers, K. D. *Adv. Drug Delivery Rev.* **2009**, *61*, 785–794.
- (49) Chang, G. T.; Yu, L.; Yang, Z. G.; Ding, J. D. *Polymer* **2009**, *50*, 6111–6120.
- (50) Yu, L.; Zhang, H.; Ding, J. D. *Colloid Polym. Sci.* **2010**, *288*, 1151–1159.
- (51) Zhang, H.; Yu, L.; Ding, J. D. *Macromolecules* **2008**, *41*, 6493–6499.
- (52) Kasperczyk, J. *Polymer* **1996**, *37*, 201–203.
- (53) Gao, Q. W.; Lan, P.; Shao, H. L.; Hu, X. C. *Polym. J.* **2002**, *34*, 786–793.
- (54) Loontjens, C. A. M.; Vermonden, T.; Leemhuis, M.; van Steenbergen, M. J.; van Nostrum, C. F.; Hennink, W. E. *Macromolecules* **2007**, *40*, 7208–7216.
- (55) Jeong, B.; Lee, D. S.; Shon, J. I.; Bae, Y. H.; Kim, S. W. *J. Polym. Sci., Part A: Polym. Chem.* **1999**, *37*, 751–760.
- (56) Gilding, D. K.; Reed, A. M. *Polymer* **1979**, *20*, 1459–1464.
- (57) Pack, J. W.; Kim, S. H.; Cho, I. W.; Park, S. Y.; Kim, Y. H. *J. Polym. Sci., Part A: Polym. Chem.* **2002**, *40*, 544–554.
- (58) Kricheldorf, H. R.; Mang, T.; Jonte, J. M. *Macromolecules* **1984**, *17*, 2173–2181.
- (59) Zhang, H.; Ding, J. D. *J. Biomater. Sci. Polymer Edn* **2010**, *21*, 253–269.
- (60) Kim, S. W.; Kim, H. J.; Lee, K. E.; Han, S. S.; Sohn, Y. S.; Jeong, B. *Macromolecules* **2007**, *40*, 5519–5525.
- (61) Yu, L.; Chang, G. T.; Zhang, H.; Ding, J. D. *J. Polym. Sci., Part A: Polym. Chem.* **2007**, *45*, 1122–1133.